

# Evaluation of antenna pattern for radiation in solid media

First Experience with an Imaging Radar arrangement

Dipl.-Ing. R. Zetik, Technical University of Košice, [zetik@tuke.sk](mailto:zetik@tuke.sk)

Dr.-Ing. J. Sachs, Technical University of Ilmenau, [sac@e-technik.tu-ilmenau.de](mailto:sac@e-technik.tu-ilmenau.de)

Dr.-Ing. B. Schneegast, MEODAT GmbH Ilmenau, [sne@meodat.de](mailto:sne@meodat.de)

## Introduction

With progress in ultra wideband system design and multidimensional signal processing, Surface-Penetrating Radar (SPR) becomes more and more interesting for industrial application also, particularly for Non-Destructive Testing in Civil Engineering (NDT-CE). The antennas as the true sensor elements are the key components of such a SPR-system. They widely determine the application field of the devices, so that a permanently increasing set of specialised sensors for the treatment of certain test problems will be available in future.

The knowledge of characteristic values which describe the radiation behaviour of SPR-antennas is of fundamental importance for the development of SPR-systems and the implementation of advanced SPR signal processing software. The well known classical descriptions of antenna properties is mostly based on power values like gain, aperture or similar and related to far-field conditions. This is a sufficient way of consideration in applications where the waves travel long distances and the relative bandwidth of the transmitted signals is not too high. The majority of communication links and free-space radar systems meet this conditions. In these cases, the antennas are considered as point sources including directional properties. This leads to a common transmission model which is easy to handle and should also be used for SPR applications because of its simplicity.

But some extensions are necessary to adapt this model for the SPR requirements. For advanced signal processing, the complete temporal and spatial antenna properties are of interest, and to retain model simplicity, it is supposed to consider the near-field behaviour by “distance dependent far-field quantities”. The last point creates some practical problems, because the measurement procedures have to be repeated several times in different distances. The temporal antenna properties can be determined by the acquisition of either real values in the time domain by classical impulse radar systems or complex values in the frequency domain by network analysers or similar equipment. From the theoretical point of view, there is no difference between both forms of consideration. The use of the Fourier-transform is a simple way to transform them one into each other. In contrast with that, the determination of the spatial behaviour or rather the angle dependent radiation properties is more complicated. A goniometer arrangement with a reference antenna is used in classical free-space measurements or for the analysis of antenna radiation in liquids. In case of radiation in a solid body, this requires a set of half-spheres consisting of the material under test (MUT) with radii that correspond to the desired (“near-field”) distances. Additionally, for absolute gain measurements, one needs a reference antenna, which has to be calibrated to the specific MUT. Another method uses a slanting bore-hole in the MUT which underpasses the antenna under test (AUT), and a reference antenna is moved inside it to sample spatial data.

The proposed procedure below to measure the antenna behaviour for radiation in a solid is aimed at

- simplifications in the realisation of the MUT, that may have a simple cubic size,
- a simple planar scanning process by using a laboratory Imaging Radar to acquire the spatial information,
- a largely automated process of data acquisition and processing to allow extensive series of experiments,
- the renunciation of a reference antenna even for absolute gain measurements,
- and the use of measurement conditions comparable to the practical applications of the SPR method which prefer bistatic antenna arrangements.

Starting from the well known relations in the (power)spectral domain, some comparable amplitude relations will be derived by complex decomposition and a “virtual bistatic antenna” is introduced. Those constitute the base for measuring and calculating the demanded values. The measuring process and the used equipment will be explained shortly. Finally first experiments will be presented. All considerations will respect to the frequency domain. See also [1] to refer to a time domain disquisition.

### Antenna characterisation by complex vector amplitudes

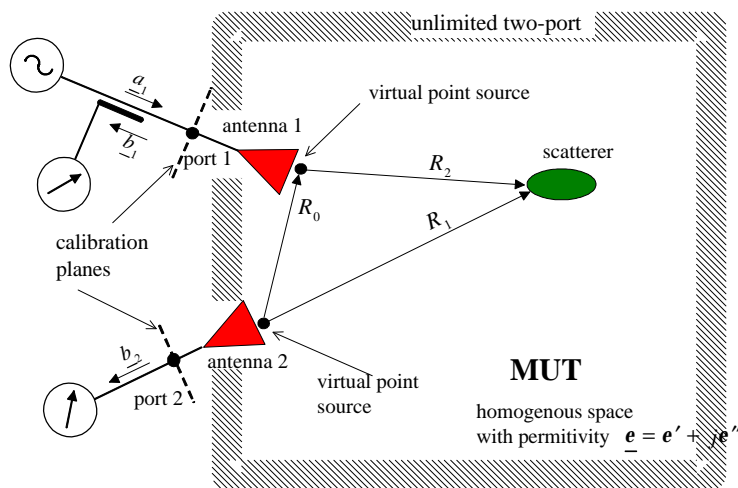


**figure 1** Antenna arrangement as a two port. The virtual point sources are characterised by  $\mathbf{h}_0$ ,  $\underline{H}(f)$ ,  $\underline{G}(f)$ ,  $\underline{Q}$  and  $\underline{\mathbf{u}}$ .

The analysis of antenna properties is always based on one or two-port measurements. Such a system consists of the AUT, and possibly, of a second antenna which are embedded in the propagation medium (MUT) (figure 1). The second antenna may be a reference one or an AUT also. As long as the antennas are not moved, the quadrupole is a LTI-system preferentially characterised by S-parameters, whose measurement can be done by a vector network analyser or time domain reflectometer. Since it is not possible to measure the antenna parameters immediately, there is a need for a model that describes the behaviour of the two-port.

For simplicity, the antennas are considered as point objects located in the vicinity of the real ones. The propagation medium consists of an unlimited space of dielectric materials which may contain one simple scatterer. According to the presence or absence of this scatterer, two different sets of S-parameters are determinable. In the power spectral domain, they can be expressed by the well known Frees formula and radar equation, respectively. Back scattering from the antennas or multiple reflections are generally omitted in this simplified considerations.

The realised gain  $G$  of the antennas is one of the important values in this relations. It relates the radiation intensity  $R^2 S$  [W/sr] in direction  $\mathbf{e}_k$  to the power incident at the antenna averaged over the unique sphere [2]. It may be expressed as follows:

$$G \mathbf{e}_k = 4\pi R^2 \frac{S \mathbf{e}_k}{\frac{1}{2} \underline{a}_1 \underline{a}_1^*} = 4\pi \frac{\mathbf{B}^* \mathbf{B}}{\underline{a}_1^* \underline{a}_1} = (1 - |\mathbf{G}|^2) \mathbf{h} D \mathbf{e}_k = 4\pi \frac{(1 - |\mathbf{G}|^2) \mathbf{h} Q \mathbf{e}_k}{\int_{4\pi} Q \mathbf{e}_k dW}. \quad (1)$$

Herein,  $\mathbf{e}_k = \underline{\mathbf{k}} / k$  is the unitary vector of the propagation direction,  $\underline{k} = k' - jk''$  is the complex wave number (norm of the wave vector  $\underline{\mathbf{k}}$ ),  $R$  is the distance between antenna and observation point,  $S$  is the power density at the observation point,  $\mathbf{h}$  is the antenna efficiency,  $D$  is the directivity, and  $Q \mathbf{e}_k = S \mathbf{e}_k / S_{\max}$  is the so called radiation pattern. The normalised far-field amplitude  $\mathbf{B}$  is shortly explained in the annex and  $\underline{a}$  is the normalised transmission line wave incident into the antenna.

Whereas the antenna gain  $G$  is a description of the transmitting mode, the effective aperture  $A_{\text{eff}}$  or receiving cross section characterises the receiving mode for incidence from direction  $\mathbf{e}_i$

$$\frac{1}{2} \underline{b}_r \underline{b}_r^* = A_{\text{eff}} Q \mathbf{e}_i S. \quad (2)$$

Applying the reciprocity relation [2],[3]

$$\underline{a}_n \underline{b}_{n,r} = -j \mathbf{I} \underline{\mathbf{A}}^* \mathbf{B} \quad (3)$$

to one of the both antennas ( $n = 1, 2$ ), the common relation between the parameters of both operation modes can be established, which is tacitly used in the common Frees and radar equations

$$A_{\text{eff},n} = \left| \frac{\underline{b}_{n,r}}{\underline{\mathbf{A}}} \right|^2 = \frac{G_n \mathbf{I}^2}{4\pi}. \quad (4)$$

Here  $\underline{b}_{n,r}$  relates only to that part of the transmission line wave, which is caused by the captured space wave and not by the electrical reflections at the antenna terminals. Comparable to normalised transmission line wave,  $\underline{\mathbf{A}} = \underline{A} \underline{\mathbf{v}}$  [ $\sqrt{W/m^2}$ ] and  $\mathbf{B} = \underline{B} \underline{\mathbf{u}}$  [ $\sqrt{W/sr}$ ] describe the vector amplitudes normalised to the intrinsic wave impedance of the propagation medium for an incident plane wave  $\underline{\mathbf{A}}$  and a radiated spherical wave  $\mathbf{B}$ , respectively.  $\underline{\mathbf{v}}$  and  $\underline{\mathbf{u}}$  are the appropriate polarisation vectors.

To get a complete frequency domain description of the antenna, the power relations described by the Frees formula and the radar equation has to be separated into complex vector amplitude relations. We can define the amplitude of the transmission line wave  $\underline{b}_r$  of a receiving antenna in a comparable manner as its open-circuit voltage by

$$\underline{b}_r = \underline{\mathbf{A}}^* \underline{\mathbf{h}}_N = \underline{A} \underline{\mathbf{v}}^* \underline{\mathbf{h}}_N \quad (5)$$

and equation (1) may be formally decomposed into a gain related vector quantity  $\underline{\mathbf{G}}_c$ <sup>1</sup>

$$\underline{\mathbf{G}}_c = \sqrt{4\pi} \frac{\underline{\mathbf{B}}}{a_1} = \sqrt{1 - |\underline{\mathbf{G}}|f|^2} \sqrt{\underline{\mathbf{h}}_0 \underline{\mathbf{H}}|f|} \frac{\underline{\mathbf{Q}}_c |e_{k,f}| \underline{\mathbf{u}}}{\sqrt{\int \underline{\mathbf{Q}}_c^* \underline{\mathbf{Q}}_c d\mathbf{W}}}. \quad (6)$$

Finally, the reciprocity relation (3) leads to

$$\underline{\mathbf{h}}_N = -\frac{j\mathbf{l}}{\sqrt{4\pi}} \underline{\mathbf{G}}_c. \quad (7)$$

In these equations  $\underline{\mathbf{h}}_N$  corresponds to the vector effective antenna length, which is normalised to the intrinsic impedances of the transmission line and the propagation medium. The direction of  $\underline{\mathbf{h}}_N$  evidently coincides with the polarisation  $\underline{\mathbf{u}}$  of the transmitted waves.  $\underline{\mathbf{h}}_0$  is the maximum antenna efficiency that occurs at the frequency  $f_0$ .  $\underline{\mathbf{H}}|f|$  characterises the frequency dependence of the efficiency as well as the internal delay and phase shift by reactive antenna elements. It is chosen in such a manner that  $\underline{\mathbf{H}}|f_0| \underline{\mathbf{H}}^*|f_0| = 1$ . The group delay of the antenna  $\underline{\mathbf{t}}_g = \nabla \arg[\underline{\mathbf{H}}|f|] / \nabla \omega$  should be largely constant within the passband in SPR applications. The radiation behaviour is given by the complex pattern  $\underline{\mathbf{Q}}_c$  and the unitary polarisation vector  $\underline{\mathbf{u}}$ , in which  $\underline{\mathbf{Q}}_c |e_{0,f}| \underline{\mathbf{Q}}_c^* |e_{0,f}| = 1$  is chosen.  $e_0$  is a reference direction, usually the direction of maximum radiation or the normal to the aperture plane of the antenna.

In the same manner as shown above, the classical Fresnel formula or the radar range equation may be expressed by complex vector amplitude relations:

$$\underline{S}_{21,0} = \frac{b_2}{a_1} = \underline{\mathbf{G}}_{c2}^* \underline{\mathbf{G}}_{c1} \frac{\mathbf{I}}{4\pi R_0} e^{-jkR_0} \quad (\text{direct transmission, complex Fresnel formula}) \quad (8)$$

$$\underline{S}_{11,S}^{(r)} = \frac{b_{1r}}{a_1} = \underline{\mathbf{G}}_{c1}^* \underline{\mathbf{C}} \underline{\mathbf{G}}_{c1} \frac{\mathbf{I}}{\sqrt{4\pi} |f|^3 R_1^2} e^{-j2kR_1} \quad (\text{monostatic radar, complex radar equation}) \quad (9)$$

$$\underline{S}_{21,S}^{(r)} = \frac{b_{2r}}{a_1} = \underline{\mathbf{G}}_{c2}^* \underline{\mathbf{C}} \underline{\mathbf{G}}_{c1} \frac{\mathbf{I}}{\sqrt{4\pi} |f|^3 R_1 R_2} e^{-jk(|R_1 + R_2|)} \quad (\text{bistatic radar, complex radar equation}) \quad (10)$$

In the equations (9) and (10) the antenna mismatch and the direct transmission (antenna coupling, breakthrough) are omitted, so that  $b_{ir}$  regards only the scattered field components. The matrix  $\underline{\mathbf{C}}$  [m] describes the reflectivity behaviour of the scatterer, relating the normalised amplitudes of the scattered spherical wave  $\underline{\mathbf{B}}_s$  to the incident plan wave  $\underline{\mathbf{A}}$  by:

$$\underline{\mathbf{B}}_s = \underline{\mathbf{C}} \underline{\mathbf{A}} \quad (11)$$

---

<sup>1</sup> The arguments  $e_k, f$  in (6) are meaningful if only a specified MUT is considered. The use of  $e_k, k$  is more general.

If the scatterer is located in the far-field of both antennas, the scattering matrix  $\underline{\mathbf{C}}$  can be reduced to a symmetric 2x2 matrix. The coefficients of this matrix depend on the incident and scattering angles as well as on the orientation of the scattering body.

## Scattering by a sphere

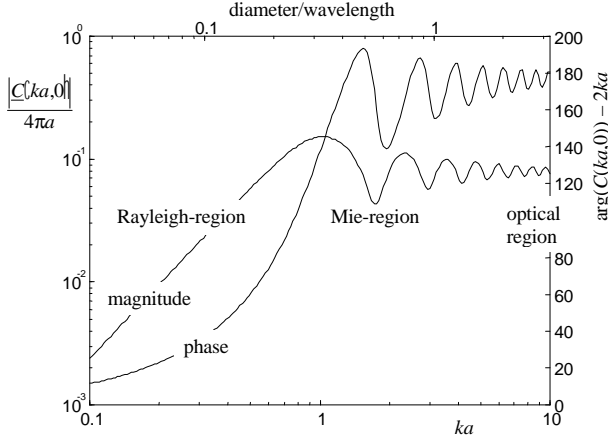


**figure 2** Magnitude and phase [deg] of the scattering coefficient for back scattering

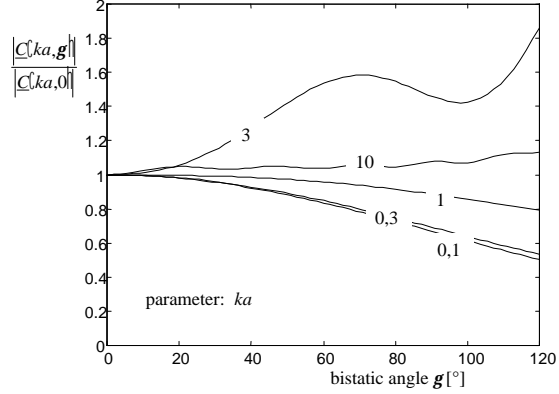


**figure 3** Relative variation of the magnitude in dependence from the bistatic angle

Equations (9) – (11) greatly simplify, if the scatterer is a sphere. For co-polarised transmission and receiving antennas ( $\underline{\mathbf{u}} = \underline{\mathbf{v}}$ ), enclosing the angle  $g$  with the scatterer,

$$\underline{\mathbf{v}}^* \underline{\mathbf{C}} \underline{\mathbf{u}} = \underline{\mathbf{C}}(ka, g) \quad (12)$$

applies in case of a sphere with radius  $a$ . The calculation of  $\underline{\mathbf{C}}(ka, g)$  for an ideal conducting sphere bases on the Mie series and is given by [6]:

$$\underline{\mathbf{C}}(ka, g) = -\frac{j}{k} \sum_{n=1}^{\infty} (-1)^n \frac{2n+1}{n(n+1)} \left\{ \begin{array}{l} \frac{\Psi_n(ka)}{\Psi_n(g)} \frac{P_n^1(\cos g)}{\sin g} - \frac{\Psi_n(ka)}{\zeta_n^{(3)}(ka)} \frac{P_n^1(\cos g)}{g} \\ \frac{\zeta_n^{(3)}(ka)}{\Psi_n(ka)} \frac{P_n^1(\cos g)}{\sin g} - \frac{\zeta_n^{(3)}(ka)}{\zeta_n^{(3)}(ka)} \frac{P_n^1(\cos g)}{g} \end{array} \right\} \quad (13)$$

$\Psi_n(x)$  - Riccati-Bessel function of first kind

$\zeta_n^{(3)}(x)$  - Riccati-Bessel function of third kind

$P_n^m(x)$  - Legendre function of the first kind, degree  $n$ , order  $m$

Magnitude and phase of the scattering coefficient for back scattering ( $g = 0$ ) are shown in figure 3. Figure 4 presents the variation of the scattering magnitude with respect to the bistatic angle  $g$ . The variation of the angle of  $\underline{\mathbf{C}}(ka, g)$  as function from  $g$  is less than  $10^\circ$  for  $g \leq 100^\circ$  ( $ka = 1$ ) and  $g \leq 20^\circ$  ( $ka = 3$ ). It is negligible for small values of  $ka$ .

The scattering strength rapidly decreases with increasing wavelength or decreasing radius. As seen in figure 3, the strong variations in the Rayleigh- and Mie-region give rise to great computation errors by even little variations of the parameters (e.g. permittivity of the MUT). Therefore it is disadvantageous to apply the scattering from a little sphere to realize absolute gain measurements. In contrast to this, the dependence of the scattering behaviour from the bistatic angle  $\theta$  is smooth in the Rayleigh- and Mie-region. It may be used for relative measurements (radiation pattern).

## What kind of parameters are important?

The equations (1) and (6) define two sets of features  $[\underline{G}(\theta, f), \mathbf{h} = \mathbf{h}_0 | \underline{H}(\theta, f)]^2, \underline{Q}_c(\mathbf{e}_k, f)]$  and  $[\underline{G}(\theta, f), \mathbf{h}_0, \underline{H}(\theta, f), \underline{Q}_c(\mathbf{e}_k, f)]$ , which basically guide antenna and SPR-system design. The equations (8) – (10) form the base of their determination.

In SPR data acquisition,  $|\underline{G}(\theta, f)|$ ,  $|\underline{H}(\theta, f)|$  and  $\mathbf{h}_0$  are the dominant design parameters, because they determine the system bandwidth and its sensitivity. The influence of the directivity with respect to the radar range is not so critical, though a high gain antenna favours it and the clutter suppression (random scatterer) also. But, the limited antenna volume and the desired bandwidth greatly restricts measures that are aimed to a wide variation range of the directivity for various antenna designs.

In SPR data processing there is an opposite situation. The knowledge of the directivity pattern is more important here, since the relations between the measurement data are of interest and not their absolute values. Two cases have to be considered. In the first one, the data interpretation is realised by practical predominant methods without use of SAFT-algorithm (synthetic aperture focusing technique). The half-power beamwidth of the antenna should be as small as possible to achieve a good cross range resolution<sup>2</sup>. A detailed knowledge of the directivity pattern is unimportant. In the second case, inverse scattering is an essential part of SPR data processing. This leads to an improved cross range resolution  $d_{cross}$  that is approximately independent from the depth of the scatterer. It is the better the larger the half-power beamwidth  $b_B$  is [4].

$$d_{cross} \cong \max \left\{ \frac{I_{min}}{2}, \frac{I_{min}}{2 \tan(b_B / 2)} \right\} \quad (14)$$

In order to achieve a cross range resolution as high as possible by exploiting SAFT-procedures or sophisticated methods of interference pattern recognition, the knowledge of the antenna parameters  $\underline{Q}_c(\mathbf{e}_k, f), \underline{H}(\theta, f)$  as well as the propagation “parameter”  $\underline{k}(\theta, f)$  of the MUT is to be supposed. A vast of NDT-CE applications is limited to a certain variation in construction materials, so that a sufficient base of the data sets  $[\underline{Q}_c, \underline{H}, \underline{k}]_{MUT}$  may considerably improve the actual processing of SPR-data.

---

<sup>2</sup> In contrast to the SAFT-methods, this resolution is an angular resolution, so that the real cross range resolution decreases with the depth of the scatterer. Moreover, it is often not the half-power beamwidth which determines the resolution but the divergence and attenuation of the waves.

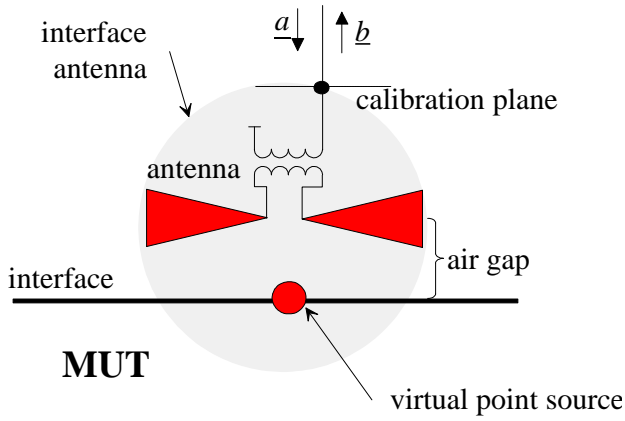


figure 4 Interface antenna

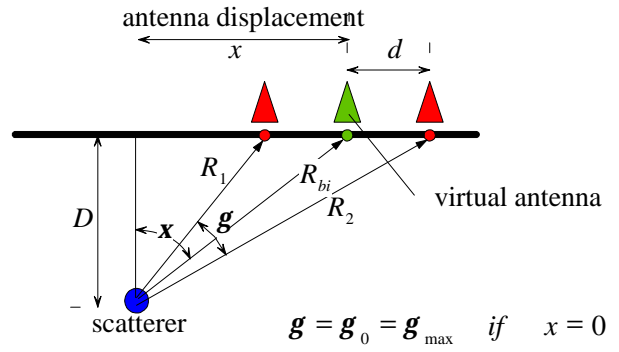


figure 5 Definition of the bistatic geometry (azimuth angle  $\mathbf{j}$  is omitted)

In many cases, SPR uses bistatic antenna arrangements in which the antennas are located at the interface between air and MUT sometimes including a small gap. Antenna, air gap and the interface form the so called interface-antenna (see figure 4). The radiation of such an antenna may be divided in three regions:

- the desired radiation into the MUT, for which the antenna should be designed,
- the radiation along the interface plane causing the breakthrough in bistatic antenna arrangements,
- and the backward radiation effecting EMC-problems and ambient clutter.

We are only interested in the radiation into the MUT, all other contributions will be counted as losses.

Finally, the radar equation (10) can be replaced by a modified monostatic one (see figure 5):

$$\underline{S}_{21,S}^{(r)} = \frac{\underline{G}_{bi}^2 \langle \mathbf{x}, \mathbf{j}, \mathbf{g}_0, k \rangle \langle \mathbf{I}, \mathbf{C} \rangle \langle k a, \mathbf{g} \rangle}{\sqrt{4\pi} \langle \mathbf{j} \rangle^3 R_{bi}^2} e^{-j2kR_{bi}} \quad \text{where} \quad \underline{G}_{bi} = \frac{\sqrt{\underline{G}_{c1} \underline{G}_{c2}}}{M} e^{-jk\Delta R} \quad (15)$$

In this case,  $\Delta R$  and  $M$  are the deviations of  $R_{bi}$  from the linear and geometric mean of the antenna distances respectively. Under this assumption the processing of mono- and bistatic radar data is identically. But apparently, considering (6) and (15), there is a difference in the number of variables in both gains. Since this is true only under far-field conditions, they are really of the same dimensional dependencies for those cases considered here.

## Estimation procedure

The estimation procedure should be aimed to determine the characteristic antenna values  $\mathbf{h}_0, \underline{H} \langle \mathbf{j} \rangle, \underline{G} \langle \mathbf{j} \rangle$  and  $\underline{Q} \langle \mathbf{x}, \mathbf{j}, f \rangle$  for different MUT's and different depths of the scatterer. Since the electrical properties of a construction material vary also with its moisture and salt content, there are many experiments necessary to characterise only one antenna arrangement. In order to perform lots of examinations an automatic measurement setup is to be preferred which is satisfied by a small MUT volume. We used a Imaging-Radar system shortly explained below and in [7]. The MUT's are simply of cubic size, and they could be sandy or solid. With regard to

several depths of a scatterer, a solid MUT has to be subdivided into a number of slices with planar surfaces to avoid air gaps if they are stacked. The complete estimation procedure can be divided into four steps.

*Step 1:* The first step consists of determining the parameters of the MUT, i.e. its complex wave number  $\underline{k}$  and the electrical reflection  $\underline{G}$ . This may be realised by radiating through the MUT.  $\underline{G}$  is got from reflection measurements where the back scattering from the opposite surface of the MUT is gated out. In connection with MUT's of different thickness, the wave number  $\underline{k}$  can be calculated from the Frees formula (8), if two antennas are situated directly opposite to the MUT. But this supposes far-field conditions and negligible reflections from the lateral surfaces. The minimum antenna distance to keep the far-field condition can be found approximately by measuring in air and increasing gradually the antenna distance until the Frees formula well predicts the measured values. If the radiation pattern, and respectively, the directivity of the antennas don't change with frequency on a large scale, the normalised transfer function  $\underline{H}(f)$  may be also estimated.

*Step 2:* This part serves to find the radiation pattern in a SPR specific manner. It is the most critical and most extensive step. Due to the introduction of a virtual bistatic antenna there is no difference in the procedure for measuring mono- or bistatic arrangements. In the following, the bistatic notation will be used only since such measurements are predominant. Obeying the proposed method a metallic sphere is buried in the MUT at a predefined depth (sphere-coordinates  $[0,0,H]$ ) and the co-polarised antennas scan in a zigzag the upper surface of the MUT (virtual antenna-coordinates  $[x,y,0]$ ). The result is a three dimensional radar volume  $\underline{S}_{21,S}(x,y,t)$  or its Fourier transform  $\underline{S}_{21,S}(x,y,f)$  as a function of the scan coordinates  $x$  and  $y$ . Regarding only those components of the radar data  $\underline{S}_{21,S}^{(r)}$  which are caused by the scattering at the sphere, equation (15) may be modified for a specific MUT and a specific sphere into the wanted relation:

$$\underline{Q}(x,j,g_0,f) = \frac{\underline{G}(x,j,g_0,f)}{\underline{G}(0,0,g_0,f)} = \frac{R_{bi}}{D} \sqrt{\frac{\underline{S}_{21,S}^{(r)}(x,y,f)}{\underline{S}_{21,S}^{(r)}(0,0,f)} \frac{\underline{C}(f,g_0)}{\underline{C}(f,g)}} e^{jk[R_{bi}-H]} \quad (16)$$

In many cases, where  $g_0$  is small, the bistatic correction in (16) may be omitted. The appropriate relations between  $x, y, R_{bi}, D, x, j, g_0$  are of simple trigonometric nature and follow from figure 5. The parasitic reflections may be separated from those of the sphere by two kinds of methods. First, the MUT is scanned two times - with and without sphere - and the difference between both radar volumes is taken, and second, the scattering hyperboloid of the sphere is gated out from the difference data. This should eliminate the second order reflections. In this way the entire upper surface of the MUT may be nearly used for the scanning process, so the dimensions of the MUT are determined by the desired maximum of  $x$  and  $j$ . The thickness of the MUT should be greater than the largest  $D$  by about the spatial expansion of the test signal. The preferable diameter of the sphere is  $0,1 \dots 1 \lambda$ , which spans one decade of bandwidth with a modest loss of measurement dynamic.

*Step 3:* The normalised transfer function  $\underline{H}_{bi}(f)$  of a bistatic antenna arrangement depends on the bistatic angle  $g_0$ , and therefore, it can not be determined by transmission measurements according to step 1. But scattering measurements suppose scatterer with a known radar cross section. It's practically out of reach for a spherical scatterer in the Rayleigh- or Mie-region.

That's why it is supposed to place a metallic foil in the same depth as the sphere and to calculate  $\underline{H}_{bi}(f)$  via image theory.

**Step 4:** Sophisticated polarimetric SPR-systems need an adequate calibration of the divers measurement channels additionally. A small strip of a metallic foil located in the depth of interest may serve as a reference. For more information it is referred to [8] and [9].

## Examples

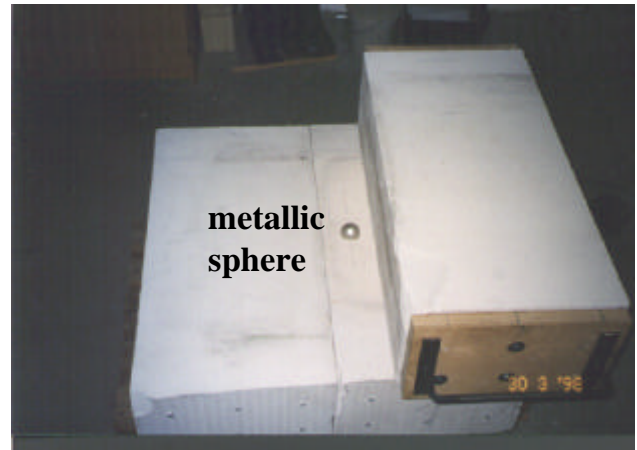
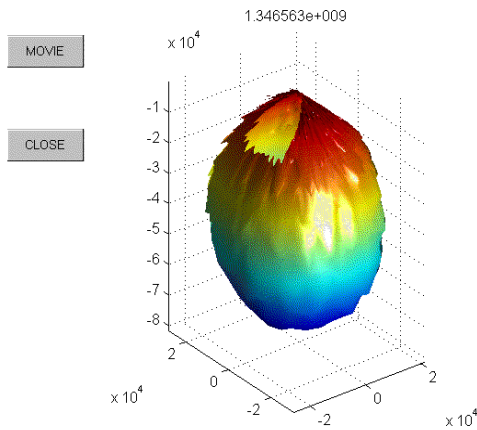


**figure 6** Magnitude of the 3D-directivity pattern of a bistatic bow-tie at 1.34 GHz

**figure 7** AAC stones showing the buried sphere

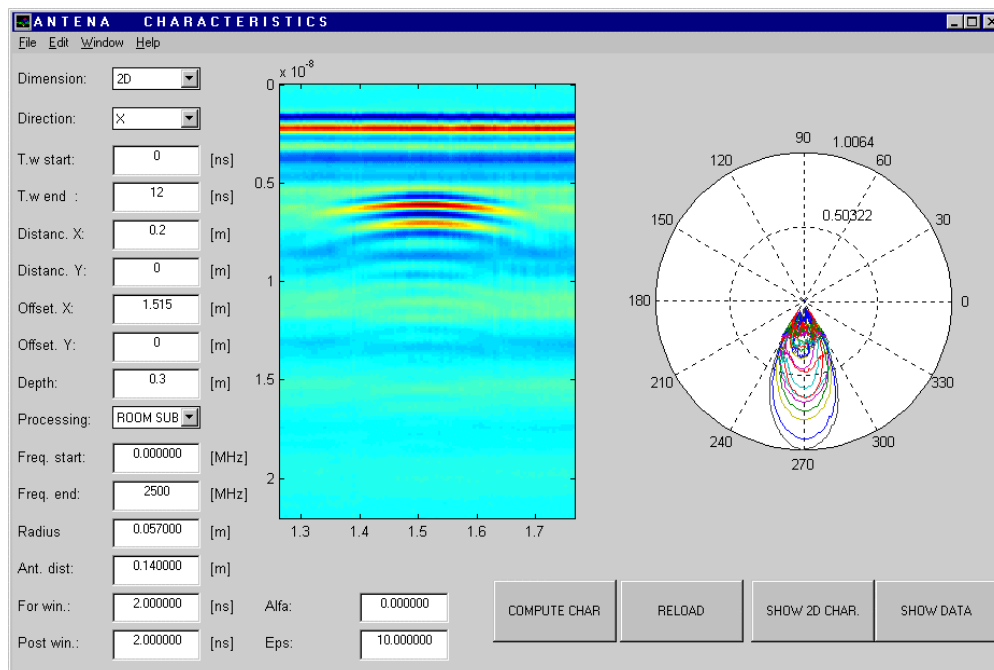


**figure 4** Hardcopy of a MATLAB panel. Only the hyperbolic section of the radar slice is used for calculating the antenna pattern.

We used an automatic radar scanner for the measurements [7]. The antenna positioning unit allows scanning an area of 2 meters times 4 meters with 0.75 mm precision and a minimum step size of 0,5 mm in both directions. With regard to a high flexibility a network analyser with

time domain option serves as a radar device. The following figures show first examples. The experiments began with radiation in air (figure 6) followed by radiation in Autoclaved Aerated Concrete (AAC) Hebel stones. Figure 7 gives an impression of the experimental details. The following figure is a hardcopy from the MATLAB panel showing a radar slice and the corresponding 2D-antenna pattern for different frequencies (not yet normalised). The radar slice is already a difference version received from measurements with and without sphere.

## Conclusion, further works

An estimation procedure was shown, which allows to determine the antenna behaviour for radiation in solid media. The antenna model bases on simple far-field considerations expanded by a radial dependence and virtual bistatic antenna. To facilitate the handling of solid MUT's and to allow measurements at different depth, the MUT's should be stacked by homogenous material slices. Further works will be directed to collect the full data set of antenna characteristics for a selected material in order to prove if this leads to better resolutions and shorter CPU-times for inverse scattering procedures.

### Annex

The normalised incident plane **A** wave may be written as:

$$\mathbf{A} = \begin{pmatrix} \mathbf{E}_i \\ \mathbf{H}_i \end{pmatrix} = \frac{\sqrt{Z} \mathbf{A}}{\sqrt{Z}} e^{-jkr} = \frac{\sqrt{Z} \mathbf{v}}{\sqrt{Z}} e^{-jkr} \quad (\text{A1})$$

In the far-field, the normalised spherical wave **B**, which leaves the virtual point source, is:

$$\mathbf{B} = \begin{pmatrix} \mathbf{E}_t \\ \mathbf{H}_t \end{pmatrix} = \frac{\sqrt{Z} \mathbf{B}}{\sqrt{Z}} \frac{e^{-jkr}}{r} = \frac{\sqrt{Z} \mathbf{u}}{\sqrt{Z}} \frac{e^{-jkr}}{r} \quad (\text{A2})$$

The product  $\mathbf{B}^* \mathbf{B} / 2 = R^2 S$  correspond to the radiated power per solid angle of the point source.

### references

- [1] A. Shlivinski, E. Heyman, R. Kastner: Antenna Characterisation in the Time Domain. IEEE AP 1997(45)7,1140-9
- [2] Y.T. Lo, S.W. Lee: Antenna Handbook Theory, Application, and Design. Van Nostrand Reinhold Comp.1988
- [3] G.A. Deschamps: II. Application du principe de r ciprocity aux antennes et aux guides d'ondes. Revue du CETHEDC (Paris), N  8-4  pp. 91-101, 1966
- [4] Warhus, J; Jeffrey, M.; Nelson, S.: Imaging Radar for Bridge Deck Inspection. [http://lasers.llnl.gov/lasers/idp/mir/files/warhus\\_spie/spiepaper.html](http://lasers.llnl.gov/lasers/idp/mir/files/warhus_spie/spiepaper.html)
- [5] D.J. Daniels: Surface-Penetrating Radar. IEE Radar, Sonar, Navigation and Avionics Series 6, 1996
- [6] J.J. Bowman, T.B.A. Senior, P.L.E. Uslenghi: Electromagnetic and Acoustic Scattering by Simple Shapes. Hemisphere Publishing Corp., 1987
- [7] R. Zetik, J. Sachs, B. Schneegast: Non-Destructive Testing with Imaging Radar: First Experience with a Laboratory Equipment. Proceedings IWK-98, Ilmenau
- [8] D.K hny, W.Wiesbeck, E.Hettlage: Vollpolarimetrischer Me platz f r r umlich aufgel ste Emissionsmessungen. 2.Int.Kongre  f r Elektromagnetische Vertr glichkeit, (M rz 1990)
- [9] F.T. Ulaby, C. Elachi: Radar Polarimetry for Geoscience Applications. Artech House 1990